Annals of Nuclear Energy xxx (xxxx) xxx

Contents lists available at ScienceDirect

Annals of Nuclear Energy

journal homepage: www.elsevier.com/locate/anucene

Whole core analysis of the single-fluid double-zone thorium molten salt reactor (SD-TMSR)

O. Ashraf [a,b,*], Andrei Rykhlevskii [c], G.V. Tikhomirov [a], Kathryn D. Huff [c]

[a] Dept. of Theoretical and Experimental Physics of Nuclear Reactors, Institute of Nuclear Physics and Engineering, National Research Nuclear University MEPhI, 31, Kashirskoe Shosse, Moscow, 115409, Russian Federation
[b] Physics Department, Faculty of Education, Ain Shams University, Cairo 11341, Egypt
[c] Dept. of Nuclear, Plasma, and Radiological Engineering, University of Illinois at Urbana-Champaign, Urbana, IL 61801, United States

ARTICLE INFO

Article history:
Received 17 May 2019
Received in revised form 20 August 2019
Accepted 9 October 2019
Available online xxxx

Keywords:
MSR
Thorium fuel cycle
Breeding reactor
Burnup
Online reprocessing
Monte carlo code

ABSTRACT

The SD-TMSR (2,250 MW_{th}) is a Single-fluid Double-zone Thorium-based Molten Salt Reactor. The active core of the SD-TMSR is divided into the inner zone (486 fuel tubes) and the outer zone (522 fuel tubes) to improve the Th-U3 breeding performance. This work adopted the SERPENT-2 Monte Carlo code to analyze the whole core model of the SD-TMSR. Built-in SERPENT-2 capabilities simulated online reprocessing and refueling and calculated the multiplication factor and Breeding Ratio (BR). We found that the molten salt Temperature Coefficient of Reactivity (α_T) was negative for initial and equilibrium states. This study investigated the variation of the multiplication factor, BR, and build-up of important nuclides in the core as a function of burnup. Under online reprocessing and refueling, we studied the variation of the reactivity during 60 years of reactor operation. Additionally, the neutron spectrum shift during the reactor operation was calculated. Finally, these simulations determined the appropriate ^{232}Th and ^{233}U feed rates for maintaining criticality and enabled analysis of the overall SD-TMSR fuel cycle performance.

1. Introduction

The Molten Salt Reactor (MSR) is the only liquid-fueled reactor that the International Forum (GIF) has chosen as one of the six promising concepts (DOE, 2002; Pioro et al., 2016). The reactor's liquid fuel distinguishes it from other nuclear reactors and allows for online reprocessing and refueling. Therefore, MSRs can potentially operate years continuously, resulting in maximum fuel utilization and high neutron economy (DOE, 2002). In an MSR, a liquid fuel salt (e.g. a mixture of $LiF–BeF_2–ThF_4–^{233}UF_4$) circulates through the core and transports fission heat to the Intermediate Heat Exchangers (IHXs). Finally, this type of reactor is expected to have a high conversion efficiency.

Both thermal and fast MSR concepts exist in the literature (Pioro et al., 2016; Engel et al., 1979). Thermal MSRs typically employ a moderator (usually graphite) to slow the neutrons down. In contrast, fast spectrum MSRs lack moderators. Liquid-fueled MSRs can breed in both cases, making them optimal for realizing desirable Th-U3 and U-Pu fuel cycles (Hargraves et al., 2010).

In the 1950s, Oak Ridge National Laboratory (ORNL) performed experiments that provided a basis for MSR feasibility. In 1958, a 5 MW_{th} homogeneous reactor experiment called HRE-2 utilized water-based liquid fuel to illustrate the intrinsic stability of homogeneous reactors. In the 1960s, ORNL performed the Molten Salt Reactor Experiment (MSRE) (Engel et al., 1979; Haubenreich and Engel, 1970; Fiorini and Leahy, 2009; Robertson et al., 1965). These experiments demonstrated the capability of circulating a liquid fluoride mixture without significant corrosion problems. Researchers used a nickel-based alloy (Hastelloy N) as structural material and controlled the fuel's oxidation by using a U^{3+}/U^{4+} buffer. The results showed that introducing noble gas bubbles into the fuel salt during operation helps extract gaseous fission products (Pioro et al., 2016).

ORNL later researched the Molten Salt Breeder Reactor (MSBR) (Rosenthal et al., 1970). There were two types of MSBR: the single-fluid molten salt reactor and the two-fluid molten salt reactor. While the single-fluid MSR dissolves fertile and fissile materials in the same salt, the two-fluid MSR physically separates them. The two-fluid MSR had a higher breeding performance than the single-fluid MSR. However, the single-fluid MSR can operate as

* Corresponding author at: Dept. of Theoretical and Experimental Physics of Nuclear Reactors, Institute of Nuclear Physics and Engineering, National Research Nuclear University MEPhI, 31, Kashirskoe Shosse, Moscow, 115409, Russian Federation.
E-mail addresses: osama.ashraf@edu.asu.edu.eg, oabdelaziz@mephi.ru (O. Ashraf).

https://doi.org/10.1016/j.anucene.2019.107115
0306-4549/

an iso-breeding reactor [1] as long as there is an efficient reprocessing system for the fuel salt (Rosenthal et al., 1970).

Despite the success of the MSRE, ORNL halted work on the MSBR in 1976. The European Atomic Energy Community (Euratom) later revived the project. To enhance the breeding performance of the MSBR, Euratom introduced the idea of dividing the core into multiple zones of fuel channels with different radii (Nuttin et al., 2005). The results showed that increasing the radii of the outer fuel channels relative to the inner radii improved the reactor's breeding and allowed it to out-perform the reactor with a single-zone core and large fuel channels (Nuttin et al., 2005).

Later, fast spectrum MSRs were introduced. Several fast MSR designs include: Molten Salt Fast Reactor (MSFR), Evaluation and Viability of Liquid Fuel Fast Reactor System (EVOL) (Serp et al., 2014), Molten Salt Actinide Recycler and Transmuter (MOSART) (Boussier et al., 2012), REBUS-3700 (Mourogov et al., 2006), and Molten Chloride Salt Fast Reactor (Taube et al., 1978). GIF has elected to further research MSFR and MOSART (Serp et al., 2014; Boussier et al., 2012; Locatelli et al., 2013; Pettersen and Mikityuk, 2016). Both designs feature the fast-spectrum, can use Th-based fuel, and liquid fuel circulation. The MSFR concept initially gained momentum at National Center for Scientific Research (CNRS) in France, and the MOSART concept is in progress in Russia.

Indeed, several challenges interfere with the commercial adoption of MSFR. For example, large initial inventory of ^{233}U and relatively long doubling time for ^{233}U production. Moreover, material scientists must identify or create structural materials which have reasonable lifespan in extreme operational conditions (high temperature, large neutron flux, chemically aggressive salt). Finally, breeding of high-quiality fissile material in the MSFR blanket rises significant nuclear non-proliferation concerns (Pettersen and Mikityuk, 2016; Merle-Lucotte et al., 2009).

The thermal MSR based on Th-U3 fuel cycle can be designed to operate with low fissile inventory and leads to a short doubling time (Zou et al., 2015). Nagy et al. studied the effect of core zoning on the breeding performance and graphite lifespan of a graphite-moderated MSR (Nagy et al., 2011; Nagy et al., 2012). Li et al. divided the active core into two zones to improve the breeding performance (Li et al., 2018). The central zone is moderated, while the unmoderated outer zone acts as a subcritical fast spectrum zone (Li et al., 2018).

In 2011, the Chinese Academy of Sciences (CAS) established the strategic project "Future Advanced Nuclear Energy – Thorium-based Molten Salt Reactor System (TMSR)". Since then, several studies aimed to improve the Thorium Molten Salt Reactor (TMSR) to efficiently utilize the Th-U3 fuel cycle (Li et al., 2018; Jiang et al., 2012; Li et al., 2015; Li et al., 2017). A number of studies have shown the fundamental possibility of organizing such a cycle in a heavy-water reactor and referred to the limitation of the burnup of solid fuels due to the accumulation of the FPs (Dastur et al., 1995, 1995.; Bergel'son et al., 2004; Bergelson et al., 2008). The question of feasibility and parameters of a Th-U3 fuel cycle in a TMSR reactor is relevant.

Liquid-fueled systems require specific neutron transport and depletion tools that capture online fuel reprocessing and refueling. Specifically, the circulation of the liquid fuel and the continuous feed or removal of elements (e.g. fissile material injection into and Fission Products (FPs) extraction from the fuel salt) are out-of-scope for most contemporary nuclear reactor physics software, which was originally written primarily to simulate solid-fueled reactors. The SERPENT-2 (Leppänen et al., 2013) code extension takes into account the online fuel reprocessing and its effects on depletion calculations (Aufiero et al., 2013).

This paper discusses the simulation of whole core depletion and continuous reprocessing of a SD-TMSR using SERPENT-2. The major objective herein is to analyze SD-TMSR neutronics and fuel cycle performance to determine the material composition at equilibrium. Additionally, we determined the major isotopes that strongly affect the core's state and compared the operational and safety parameters of the SD-TMSR at both initial and equilibrium states. Finally, these simulations determined the appropriate ^{232}Th and ^{233}U feed rates for maintaining criticality and enabled analysis of the overall SD-TMSR fuel cycle performance. All calculations presented in the present work were implemented using SERPENT-2 version 2.1.30. We adopted the MSR burnup routine provided by SERPENT-2 to simulate continuous online reprocessing and refueling in contrast with other batch-wise codes [2] (e.g. SaltProc (Rykhlevskii et al., 2019) and MCNP6-PYTHON (Jeong et al., 2016)). SERPENT-2 uses an internal calculation routine for solving the set of Bateman equations describing the changes in the material compositions caused by neutron-induced reactions and radioactive decay (Leppänen et al., 2013). Moreover, SERPENT-2 allows us to conduct the burnup calculations on computer clusters with multiple cores using distributed-memory MPI parallelization. The drift of the delayed neutron precursors is not examined in this paper, but discussion about this factor can be found in Zhang et al. (2018).

The present paper is organized as follows: after a general introduction about MSR systems, Section 2 briefly presents the Single-fluid Double-zone Thorium-based Molten Salt Reactor (SD-TMSR). Section 3 focuses on the methodology and calculation tools used in this work. Fission products extraction modeling is described in Section 4. Section 5 highlights the results and discussion. Finally, Section 6 summarizes the conclusions.

2. SD-TMSR model description

The SD-TMSR (Li et al., 2018; Mathieu et al., 2006) is a Single-fluid Double-zone Thorium-based Molten Salt Reactor. The active core is divided into the inner zone (486 fuel tubes) and the outer zone (522 fuel tubes) to improve Th-U3 breeding performance.

Fig. 1 shows the half longitudinal section of the reactor and Fig. 2 shows the plan view of the whole-core configuration. The active core is a cylinder with diameter and height equal to 460 cm. Assemblies of graphite[3] hexagonal prisms with side length 7.5 cm fill the core. The fuel channel pierces the graphite hexagonal prisms. The radius of the fuel tubes in the inner zone is 3.5 cm and the radius of the fuel tubes in the outer zone is 5 cm. Both axial and radial reflectors surround the active core to decrease the neutron leakage and enhance neutron economy (i.e. maximize neutron flux). The graphite radial reflector is 50 cm thick and the axial reflector is 130 cm in height.

The composition of the fuel salt in the present study is 70LiF - 17.5BeF_2–12.5(HM[4]) F_4 mole%. The density of the fuel salt is 3.3 g/cm^3 and the operating temperature is 900 K. The total fuel volume is 52.9 m^3 and it is considered single-fluid to simplify reprocessing. The feed rate of ^{232}Th and ^{233}U is adjusted to maintain criticality. In addition, the enrichment of ^{7}Li is 99.995% to minimize capture in ^{6}Li.

The fuel salt circulates through the tubes in the center of the graphite assemblies from bottom to top and mixes in the upper

[1] Iso-breeding reactor refers to a reactor with conversion ratio = 1, thus self-sustaining with natural Th and/or U as only feed.

[2] In the batch-wise technique, the simulation stops at a certain time and restarts after removing of poisoning isotopes and addition of fissile and/or fertile materials.

[3] We choose graphite density of 2.3 g/cm^3, to validate our results against results in the literature (Li et al., 2018; Nuttin et al., 2005).

[4] HM is Heavy Metal (i.e. ^{232}Th and ^{233}U) in this study

Please cite this article as: O. Ashraf, A. Rykhlevskii, G. V. Tikhomirov et al., Whole core analysis of the single-fluid double-zone thorium molten salt reactor (SD-TMSR), Annals of Nuclear Energy, https://doi.org/10.1016/j.anucene.2019.107115

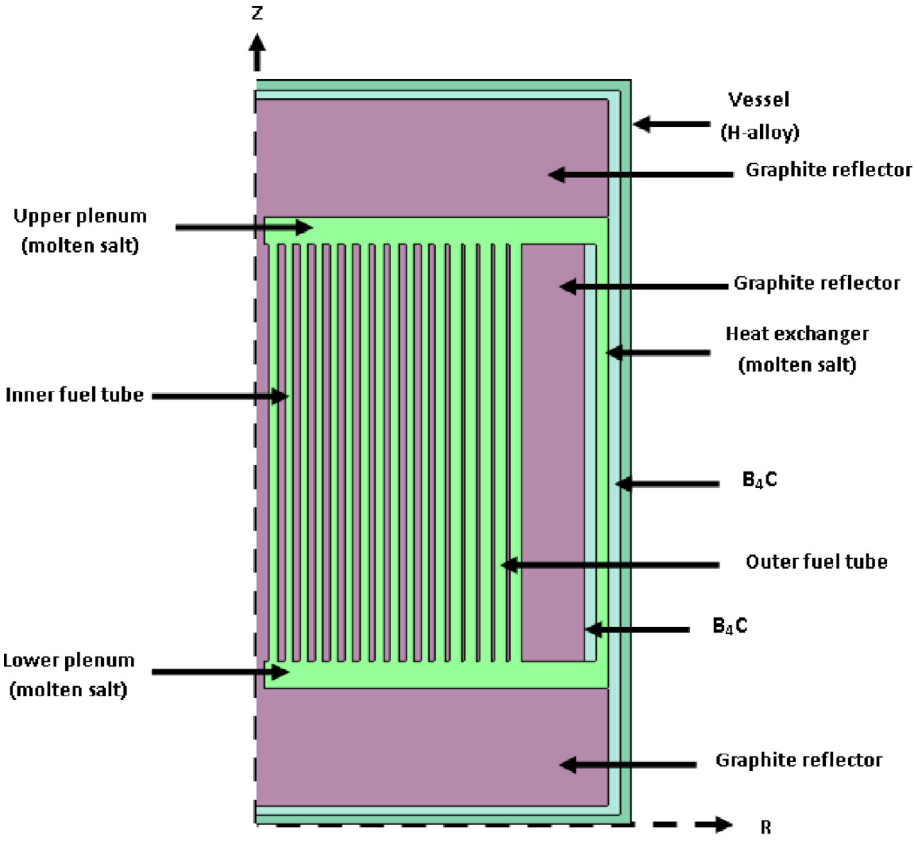

Fig. 1. Analyzed SD-TMSR geometry.

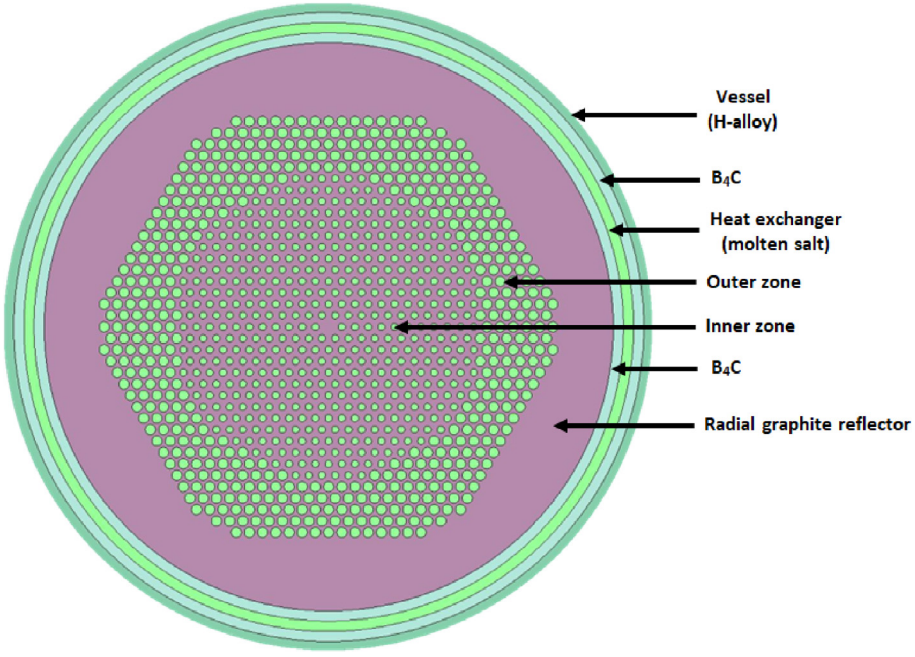

Fig. 2. Plan view of SD-TMSR core.

plenum. Then onward the pumps and the intermediate heat exchangers. Finally, the fuel returns to the lower plenum and the cycle begins again. The fuel salt continuously circulates and removes fission heat from the core to the IHX. The core is surrounded by a 10-cm-thick B_4C cylinder (density of B_4C is 2.52 g/cm^3 and enrichment of ^{10}B is 18.4%). Another 10-cm-thick cylinder made of a Ni-based (hastelloy) surrounds the whole core. During normal operation, the B_4C acts as a shield against neutrons and heat; the hastelloy provides structure and heat protection. The main characteristics of the SD-TMSR are summarized in Table 1.

The volume ratio of the fuel salt to the graphite moderator plays a significant role in controlling breeding performance. The optimal

Please cite this article as: O. Ashraf, A. Rykhlevskii, G. V. Tikhomirov et al., Whole core analysis of the single-fluid double-zone thorium molten salt reactor (SD-TMSR), Annals of Nuclear Energy, https://doi.org/10.1016/j.anucene.2019.107115

Table 1
The main characteristics of the SD-TMSR (Li et al., 2018).

Thermal power, MW_{th}	2,250
Fuel salt components	LiF–BeF_2-(HM) F_4
Fuel composition, mole%	70–17.5–12.5
^{7}Li enrichment, %	99.995
Fuel temperature, K	900
Fuel density at 900 K, g/cm^3	3.3
Fuel dilatation coefficient, g/(cm^3.K)	-6.7×10^{-4}
Graphite density, g/cm^3	2.3
B_4C density, g/cm^3	2.52
^{10}B enrichment, %	18.4
Core diameter, cm	460
Core height, cm	460
Side length of the graphite hexagonal prism, cm	7.5
Inner radius, cm	3.5
Outer radius, cm	5
Ratio of molten salt and graphite in the inner zone	0.357
Ratio of molten salt and graphite in the outer zone	1.162
Fuel volume, m^3	52.9

radius of the fuel channels in both inner and outer zones, as well as the side length of the graphite hexagonal prisms, were investigated and determined in Li et al. (2018).

3. Methodology and calculation tools

Although many neutron transport tools can model solid-fueled reactors, they often lack key capabilities for modeling liquid-fueled systems. MSR development requires us to diversify essential computational codes for modeling and simulating them. Liquid-fueled systems present two main challenges: (1) liquid salt flow and (2) an online reprocessing system (Ashraf et al., 2018; Betzler et al., 2017). To more accurately analyze MSR systems, computational codes must support online fuel salt reprocessing and refueling (Serp et al., 2014). For instance, the SCALE (DeHart and Ulses, 2006; Bucholz et al., 1982) package has the TRITON control module which couples KENO or NEWT with ORIGEN-S (Ade, 2012), also MCNP (Briesmeister et al., 2000) coupled with ORIGEN 2.2 through Monteburns (Trellue and Poston, 1999) or VESTA (Davidson et al., 2018; Haeck, 2012). SERPENT-2 (Leppänen et al., 2013) is a Three Dimensions (3D) continuous energy Monte Carlo neutron transport and burnup code. The extension accounts for continuous online reprocessing and refueling (Aufiero et al., 2013). This study utilizes SERPENT-2 to analyze fuel depletion of the SD-TMSR core with online reprocessing and refueling. ENDF/B-VII.0 was used to collect continuous microscopic cross-section data. The results reflect full-core runs of 12.5 million neutron history per burnup step. The full operation time of the reactor was 60 years (507.34 *MWd/kgHM*) with statistical uncertainty in k_{eff} equal to ± 35 *pcm*. Removing Fission Products (FPs) and noble gases online provides many advantages for MSRs. For instance, it would enhance the breeding performance and reduce the fissile inventory required to maintain criticality. The criticality can be achieved during burnup by the online feed of ^{233}U and/or ^{232}Th. Fig. 3 illustrates a flow chart of the calculation procedures.

As shown in Fig. 3, the first step included preparing and running the SERPENT-2 input file containing the geometry and material definition. Within SERPENT-2, an advanced matrix exponential solution depending on the Chebyshev Rational Approximation Method (CRAM) (Isotalo and Pusa, 2016) helped to solve the Bateman equation. Meanwhile, the system removed gaseous FPs and other materials (non-dissolved metals, lanthanides, and soluble metals except protactinium) on suitable time scales.[5] This can be done by adjusting the flow rate of gaseous FPs and other materials from the fuel to the `FP-waste tank`[6]. In specific, protactinium was extracted from the core with a certain flow rate into the external tank, `pa-tank`[7], to decay and produce ^{233}U [8].

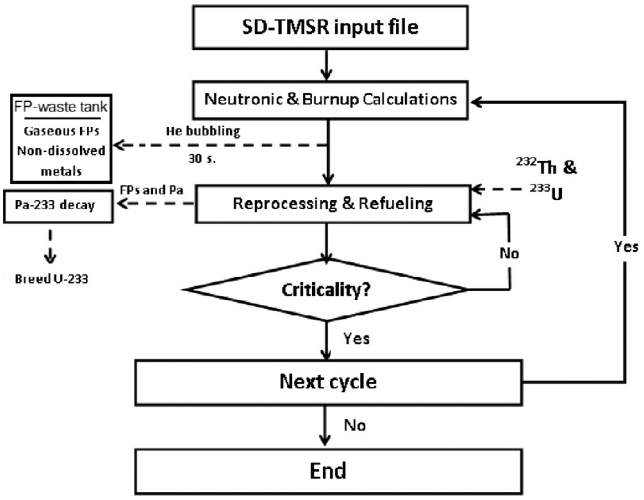

Fig. 3. Flow chart of the calculation procedures.

The MSR burnup routine has been used in this work. In order to deal with this routine, we have to determine the mass flow (*mflow*), which is the rate by which elements or nuclides are transferred between materials. After that, the transfer rates should be connected to materials with a reprocessing scheme. Finally, we have to link the reprocessing schemes to depletion histories. In the present work, we adjusted the transfer rates of fresh fuel to maintain core criticality and to keep fuel salt inventory constant during burnup. The feed constant calculation procedures are summarized as follows:

1. The simulation started without any injection of refueling materials (i.e. with only removing of FPs and Pa).
2. After first depletion calculation step, we checked the total mass density of FPs and Pa in `FP-waste tank` and `pa-tank`, respectively.
3. A simple calculation yields the amount of Th and ^{233}U that must be added during this cycle (mass of Th $\approx$ mass of extracted FPs and mass of ^{233}U $\approx$ mass of extracted Pa).
4. Dividing this mass by time and inventory of refueling material gave the corresponding feed constant (see Table 3).

The cycle calculation ran iteratively until the burnup reached the desired worth.

4. Feed rates and FP extraction

The FPs act as neutron poisons; they powerfully affect the reactor's behavior. The MSR should extract FPs during operation. Consider T_r as the time during which the whole salt is reprocessed and dN_e as the amount of specific element e with inventory N_e that the MSR extracts during time dt; therefore (Nuttin et al., 2005)

$$\frac{dN_e}{dt} = N_e \frac{\varepsilon_e}{T_r}, \tag{1}$$

[5] The extraction time depends on the type of material and its impact on the neutron economy.

[6] An imaginary tank used to store the gaseous FPs and the other FPs except protactinium.

[7] An imaginary tank used to store protactinium extracted from the core.

[8] The ^{233}Pa is removed and left to decay into ^{233}U with $\tau_{1/2} \approx 27$ *d*.

Please cite this article as: O. Ashraf, A. Rykhlevskii, G. V. Tikhomirov et al., Whole core analysis of the single-fluid double-zone thorium molten salt reactor (SD-TMSR), Annals of Nuclear Energy, https://doi.org/10.1016/j.anucene.2019.107115

Table 2
The reprocessing table.

Reprocessing group	Element	Reprocessing time	Removal constant λ_e [s^{-1}]
Gaseous FPs and non-dissolved metals	H, He, N, O, Ne, Ar, Kr, Nb, Mo, Tc, Ru, Rh, Pd, Ag, Sb, Te, Xe, Lu, Hf, Ta, W, Re, Os, Ir, Pt, Au and Rn.	30s	−3.333E−02
Lanthanides and other soluble FPs	Zn, Ga, Ge, As, Se, Br, Rb, Sr, Y, Zr, Cd, In, Sn, I, Cs, Ba, La, Ce, Pr, Nd, Pm, Sm, Eu, Gd, Tb, Dy, Ho, Er, Tm and Yb.	10.599 d (5 m^3/d)	−1.092E−06
Protactinium	Pa	10.599 d (5 m^3/d)	−1.092E−06

Table 3
The refueling table.

Nuclide	Feed rate	Feed constant* λ_e [s^{-1}]
^{232}Th	1.842 [kg/day], first 90 [d]	1.500E−09
	2.511 [kg/day], from 90 to 1550 [d]	2.045E−09
	2.456 [kg/day], from 1550 to 3010 [d]	2.000E−09
	2.321 [kg/day], from 3010 to 5930 [d]	1.890E−09
	2.241 [kg/day], from 5930 to 7390 [d]	1.825E−09
	2.186 [kg/day], from 7390 to 12500 [d]	1.780E−09
	2.118 [kg/day], from 12500 to 15420 [d]	1.725E−09
	2.136 [kg/day], from 15420 to 18340 [d]	1.740E−09
	2.063 [kg/day], from 18340 to 21900 [d]	1.680E−09
^{233}U	2.619 [kg/day], first 90 [d]	6.400E−09
	2.009 [kg/day], form 90 to 1550 [d]	4.910E−09
	1.944 [kg/day], from 1550 to 3010 [d]	4.750E−09
	1.826 [kg/day], from 3010 to 5930 [d]	4.460E−09
	1.811 [kg/day], from 5930 to 7390[d]	4.425E−09
	1.744 [kg/day], from 7390 to 12500 [d]	4.260E−09
	1.699 [kg/day], from 12500 to 18340 [d]	4.150E−09
	1.657 [kg/day], from 18340 to 21900 [d]	4.050E−09

* Feed constant is the mass fraction of fertile or fissile nuclides (^{232}Th or ^{233}U) transferred from the external storage to the core per second.

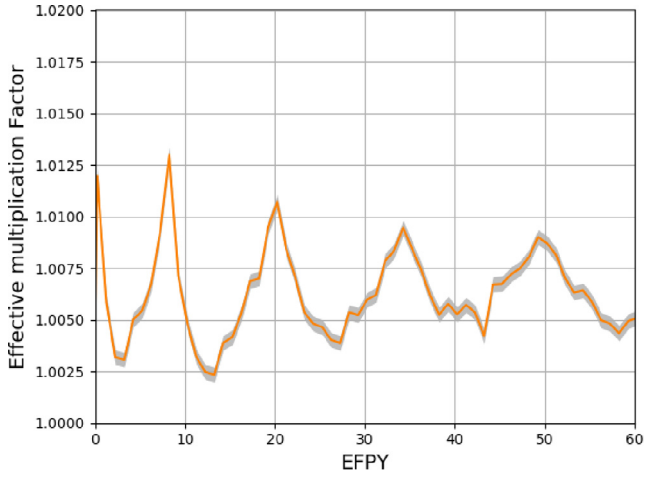

Fig. 4. The change of the effective multiplication factor during 60 EFPY of reactor operation including periodic fissile material insertion (confidence interval $\pm\sigma$ is shaded).

where ε_e is the extraction efficiency. Integrating Eq. 1 introduces a new parameter called the removal constant $\lambda_e = \varepsilon_e / T_r$. For simplicity, ε_e is considered to be 100%; thus λ_e is inversely proportional to T_r. Table 2 lists the removal constants of the gaseous FPs and other materials (non-dissolved metals, lanthanides, and soluble metals). The effective reprocessing time for the gaseous FPs and non-dissolved metals was set to 30 s (removal constant $\lambda_e = -0.0333\ s^{-1}$), because such elements ought to be removed quickly and continuously via a gas bubbling system. In contrast, extracting the other soluble FPs and lanthanides should occur by the chemical reprocessing system. Therefore, the system reprocesses a small amount of molten salt every day. The effective reprocessing time for soluble FPs lasts ≈10.59 days ($\lambda_e = -1.092 \times 10^{-6}\ s^{-1}$), which is equivalent to a chemical reprocessing rate of 5 m^3/d (Nuttin et al., 2005; Li et al., 2018). A chemical reprocessing system extracts protactinium with the same reprocessing time as the soluble FPs (i.e. 10.59 days); however, the protactinium is extracted into another tank, `pa-tank`, and left to decay. The produced ^{233}U is used as a fresh fuel and the residual ^{233}U is the net production ^{233}U. The effective feed rates of the ^{232}Th and ^{233}U are changed with burnup to keep the reactor critical and conserve the total mass of the fuel salt. Table 3 highlights the effective feed rates of ^{232}Th and ^{233}U.

5. Results and discussion

5.1. Steady-state calculation

The present study focused on the 2,250 MW_{th} SD-TMSR design. According to the optimization results from Li et al. (2018), the radius of the fuel tubes in the inner and outer zones is adjusted to 3.5 and 5 cm respectively. Similarly, the side length of the hexagonal prism (graphite) is set to 7.5 cm. The ratio between the molten salt volume and graphite volume in the inner and outer zones is 0.357 and 1.162 respectively. At the steady-state calculation, to achieve criticality (i.e. k_{eff} = 1.00469±0.00035), the start-up molten salt fuel is adjusted to LiF-BeF_2-ThF_4-$^{233}UF_4$ at 70–17.5–12.3–0.2 mol%. Accordingly, the initial (corresponding) inventory of ^{233}U and ^{232}Th are 1.3 and 76.87 tons, respectively. The Breeding Ratio (BR) at the start-up time is the ratio of total ^{232}Th capture rate to total ^{233}U absorption rate[9]. Notably, the breeding ratio does not capture any losses in the Pa separations and recycling process. The BR calculated by SERPENT-2 code at the steady state is 1.11658±0.00060. These findings agree with published data (Li et al., 2018).

5.2. Fuel depletion analysis

To gain a better understanding of the effect of online reprocessing and refueling on the performance of the SD-TMSR, the present work investigated fuel depletion in the reactor taking online reprocessing and refueling into account. The MSR burnup routine provided by Monte Carlo code SERPENT-2 simulated online reprocessing. The chemical reprocessing rate was set to 5 m^3/d and simulation time was set to reactor lifetime (60 years). Fig. 4 represents the effective multiplication factor as a function of Effective Full-Power Years [EFPY]. The effective multiplication factor fluctuates in a very narrow region (less than 1000 *pcm*). In addition, the effective multiplication factor increases by only 0.025% at the end of the operation lifetime.

During the full operation time, the reactor maintained criticality by adjusting the feed or refill rate of ^{233}U as listed in Table 3. Fig. 5 shows the variation of the reactivity during 60-years of reactor operation. The change in the reactivity was calculated at the end

[9] At the start-up time for the Th-U3 fuel cycle, fuel salt contains only ^{232}Th and ^{233}U.

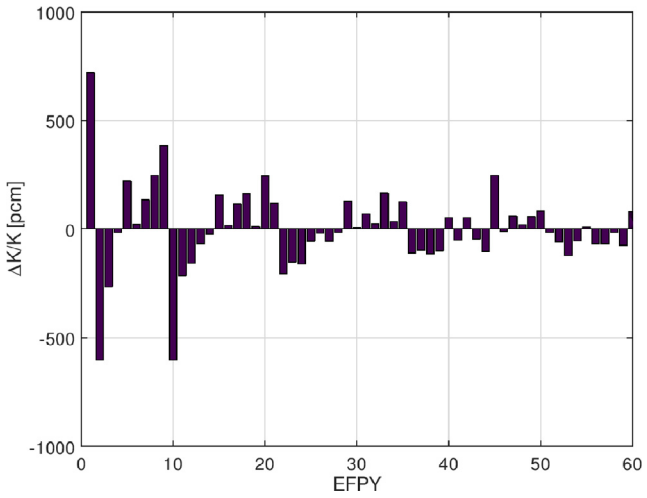

Fig. 5. The change of the reactivity during 60 EFPY of reactor operation.

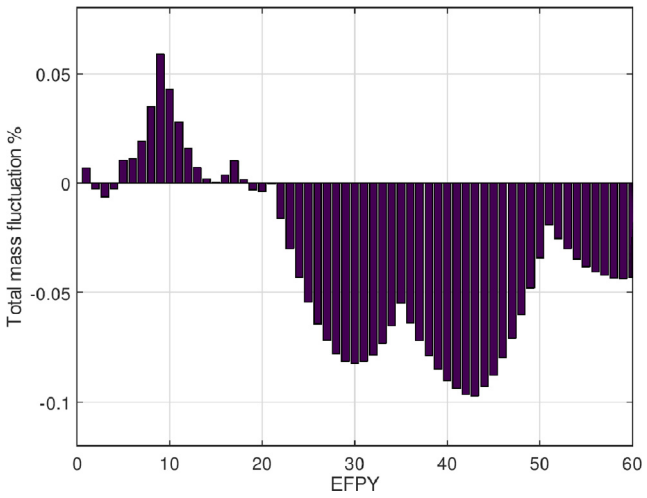

Fig. 7. Fluctuation of the total fuel mass during burnup period (60 EFPY).

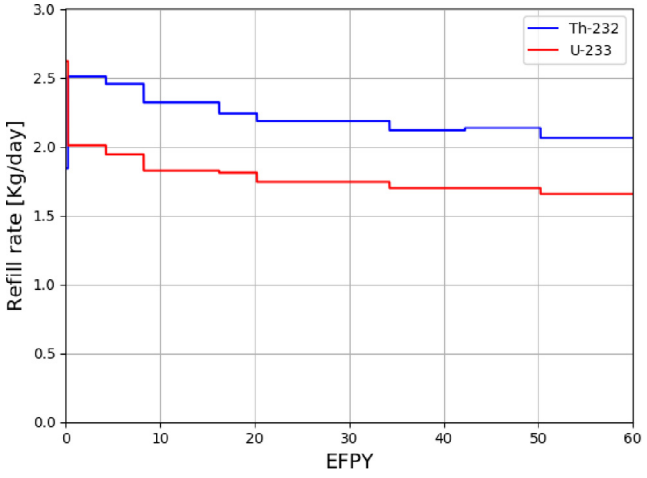

Fig. 6. Dynamics of ^{233}U and ^{232}Th refill rate during 60 EFPY of SD-TMSR operation at 100% power level.

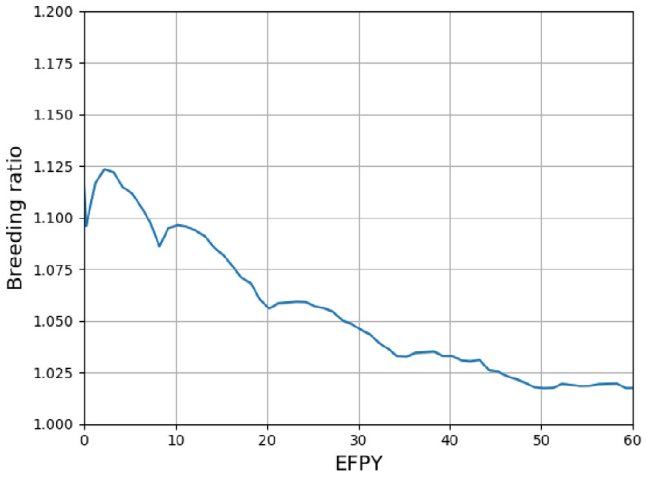

Fig. 8. The variation of the breeding ratio BR during 60 EFPY of reactor operation.

of every time step. The negative values do not mean that k_{eff} dropped below 1.0, but that k_{eff}[10] has decreased. The maximum increase in reactivity is 720 *pcm*. This reflects the possibility of controlling the reactor by changing the flow rate of fissile and fertile materials.

Fig. 6 illustrates the variation of the refill rate of ^{233}U with time. The excess reactivity has been controlled by decreasing the refill rate of ^{233}U with time as shown in Fig. 6. The maximum ^{233}U add rate was 2.62 kg/d throughout the first 90 *d*, and the mean value was 1.77 kg/d throughout 60 years of operation.

Fig. 7 demonstrates the fluctuation of the total fuel mass during the reactor lifetime. The variation of the total fuel mass is less than 0.1% during the full reactor lifetime, which agrees with early MSBR research (Rykhlevskii et al., 2019). To keep the total fuel mass variation below 0.1% throughout the burnup period, the refill rate of ^{232}Th is adjusted as listed in Table 3. Fig. 6 illustrates the variation of the feed rate of ^{232}Th with time. The maximum ^{232}Th refill rate was 2.51 kg/d in the interval from 90 to 1550 d, and the mean value was 2.21 kg/d throughout 60 years of operation. This result agrees with Rykhlevskii et al. (2019).

Fig. 8 displays the breeding ratio BR as a function of burnup. The BR is $\geqslant$1.0 during the whole depletion period. However, Fig. 8 shows that BR decreases over time. This may be attributed to the change in the capture rate of the FPs and transuranic elements[11] (Merle-Lucotte et al., 2008). Meanwhile, accumulation of non-fissile strong neutron absorbers (for instance ^{234}U and ^{149}Sm) affects the BR (see Fig. 8). Notably, the breeding configuration of this design is not strictly necessary since it could be designed as a breakeven reactor. Fig. 9 represents the total mass of the elements in the `pa-tank`. The total mass of the protactinium and its daughters in the `pa-tank` at the end of the reactor operation lifetime (60 years) reaches about 40.5 *t*. The major isotope in the `pa-tank` is ^{233}U (40.4 *t*). This helps to estimate the mass of extracted protactinium and calculate ^{233}U feed rate. Likewise, Fig. 9 illustrates the total mass of the extracted elements[12] in the `FP-waste tank`. After 60 years, this value reaches about 51 *t*. Therefore, multiple storage tanks are needed. The total mass of refueled ^{232}Th and ^{233}U compensates for the extracted elements. Therefore, the total fuel mass remains almost constant during the burnup (see Fig. 7).

[10] During the full reactor operation lifetime the k_{eff} was $\geqslant$1.002.

[11] transuranic elements are those elements with atomic numbers >92.

[12] Non-dissolved metals, lanthanides, and soluble metals except protactinium.

Please cite this article as: O. Ashraf, A. Rykhlevskii, G. V. Tikhomirov et al., Whole core analysis of the single-fluid double-zone thorium molten salt reactor (SD-TMSR), Annals of Nuclear Energy, https://doi.org/10.1016/j.anucene.2019.107115

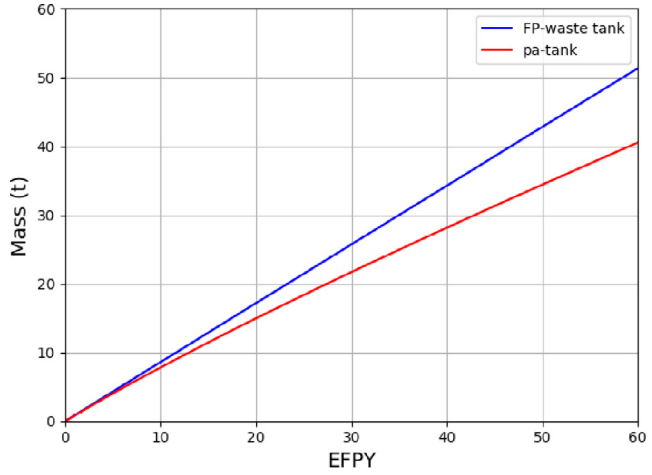

Fig. 9. Total mass of the protactinium and its daughters in the `pa-tank` (red) and extracted fission products in the `FP-waste tank` (blue). (For interpretation of the references to colour in this figure legend, the reader is referred to the web version of this article.)

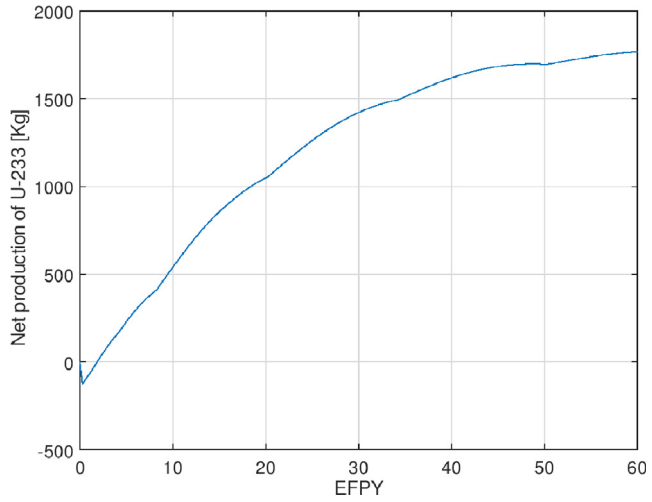

Fig. 10. Net production of ^{233}U during burnup period (60 EFPY).

It is supposed that the reactor uses ^{233}U from the `pa-tank` as fresh fuel. The difference between the amount of refueled ^{233}U into the core and the amount of ^{233}U in the `pa-tank` in every step is the net production of ^{233}U. Fig. 10 represents the net production of ^{233}U during the considered operational time. The net production of ^{233}U increases with burnup and reaches about 1.77 *t* at the end of 60 years. According to Fig. 10, after 26 years, the net production of ^{233}U reaches 1.3 *t*, which is sufficient to start-up another SD-TMSR. Fig. 10 also shows that the net production of ^{233}U during the first 455 days is negative. Therefore about 175.28 *kg* of ^{233}U must be added during this period. The negative net production of ^{233}U may be attributed to the fact that the `pa-tank` does not include ^{233}U at the beginning of the reactor lifetime.

Fig. 11 describes the evolution of major isotopes that strongly affect the core's state. The mass of protactinium in the fuel salt reaches 17.8 kg at the end of the operation period; however, the total mass of the isotopes (protactinium and its decay products) in the `pa-tank` reaches 40.5 *t* in the same period. The ^{233}Pa absorbs a neutron to become ^{234}Pa, which decays to ^{234}U. This leads to a decrease in the net production of ^{233}U. Thus, a large amount of protactinium is extracted from the core to the `pa-tank`. The protactinium reaches the equilibrium state quickly. In

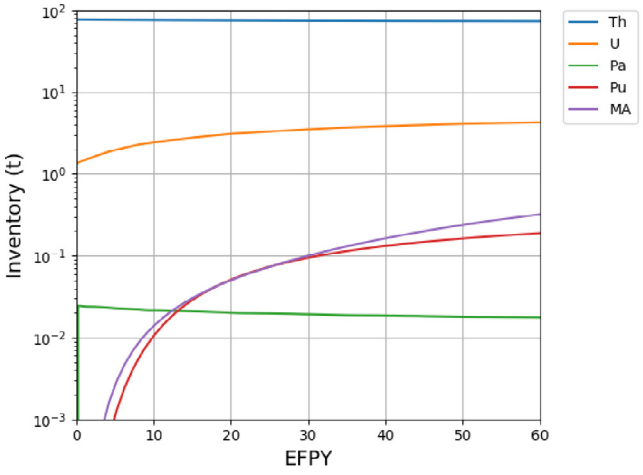

Fig. 11. Inventory of important nuclides over 60-EFPY depletion (MA involves Np, Am, and Cm).

addition, the total mass of minor actinides (MAs) [13] increases over time. However, by adopting online reprocessing, its value remains relatively low. Similarly, the total mass of Pu increases with reactor operation time. The level of Pu in the core correlates with the mass of the MA. However, MAs need more time to reach equilibrium than protactinium. The total mass of U increases with time and reaches equilibrium after about 27 years. As shown in Fig. 11, refueling the reactor with Th helps maintain an almost constant inventory throughout the full operation time.

Fig. 12 describes the variation of the ^{233}U and ^{232}Th mass with burnup. After about 10 years, the change in ^{233}U mass falls below 1%. In addition, the change in ^{232}Th mass is less than 1% during the whole depletion period. This helps to determine the equilibrium fuel salt composition (where equilibrium is defined as periods when the number densities of major isotopes vary by less than 1% over several years) (Rykhlevskii et al., 2019).

Fig. 13 illustrates the evolution of ^{234}U and ^{235}U isotope in the core. ^{234}U is an undesirable, non-fissile strong neutron absorber. Therefore, the ^{233}Pa is extracted and left to decay into ^{233}U far from the reactor core to avoid excess production of ^{234}U. Meanwhile, the fissile isotopes (for instance ^{235}U) accumulate in the core as shown in Fig. 13.

5.3. Neutron spectrum

Fig. 14 represents the neutron flux per unit lethargy for whole-core SD-TMSR model in the energy range from 10^{-9} to 10 MeV at initial state, 8, 16, 20, 22 and 24 years. After 20 years, the spectrum is almost constant; hence, equilibrium is achieved at 20 years. At the equilibrium state, the neutron spectrum is harder than at initial state due to the accumulation of the plutonium and other strong thermal neutron absorbers in the core throughout the burnup period. The spectrum for initial and equilibrium state agrees with previous research for a similar thermal-spectrum thorium-fueled MSBR design (Rykhlevskii et al., 2017).

5.4. Neutron flux

Figs. 15, 16 show the spatial distribution of fast and thermal neutron flux[14] for the initial and equilibrium (after 20 years of

[13] In the present work, the Minor Actinides (MA) include Np, Am, and Cm.

[14] For the fast neutron flux, we assumed energy range from 0.625 eV to 20 MeV, and for the thermal neutron flux from 10^{-5} eV to 0.625 eV.

Please cite this article as: O. Ashraf, A. Rykhlevskii, G. V. Tikhomirov et al., Whole core analysis of the single-fluid double-zone thorium molten salt reactor (SD-TMSR), Annals of Nuclear Energy, https://doi.org/10.1016/j.anucene.2019.107115

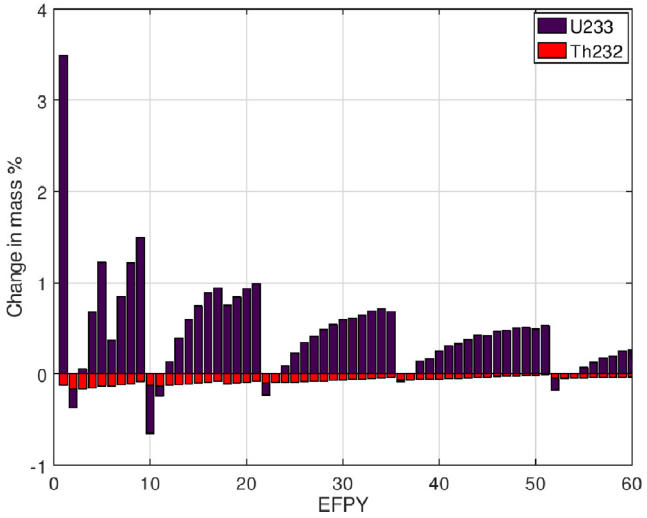

Fig. 12. Variation of ^{233}U and ^{232}Th mass over 60-EFPY depletion.

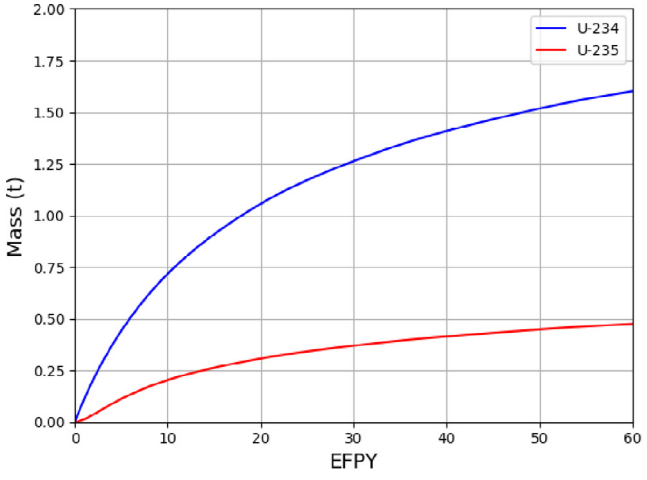

Fig. 13. Build-up of ^{234}U and ^{235}U over 60-EFPY depletion.

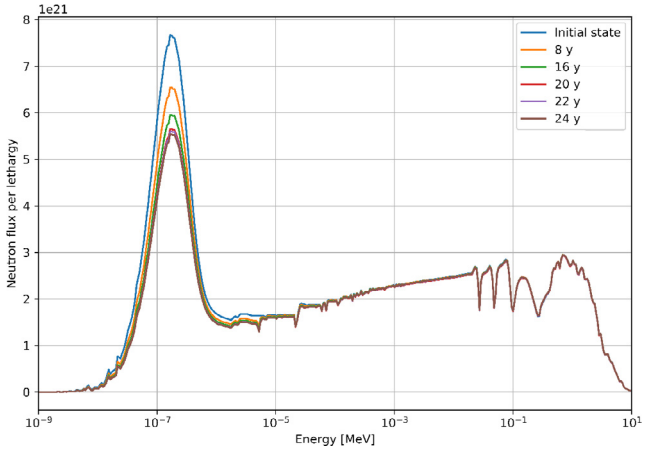

Fig. 14. The neutron flux energy spectrum at different time step.

operation) compositions. Total and thermal neutron fluxes are suppressed at the equilibrium state due to actinide evolution in the fuel salt. Specifically, fissile ^{233}U in the core is gradually substituted with heavier fissile isotopes: ^{235}U, ^{239}Pu, and ^{241}Pu. These isotopes have larger fission cross-sections and neutron yields than ^{233}U

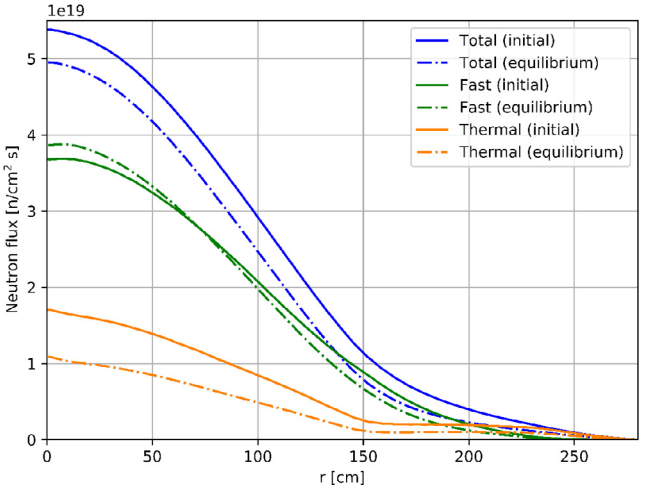

Fig. 15. Radial neutron flux distribution for initial and equilibrium fuel salt composition (the total flux confidence intervals $\pm\sigma$ are 0.6398% and 0.6199%, respectively).

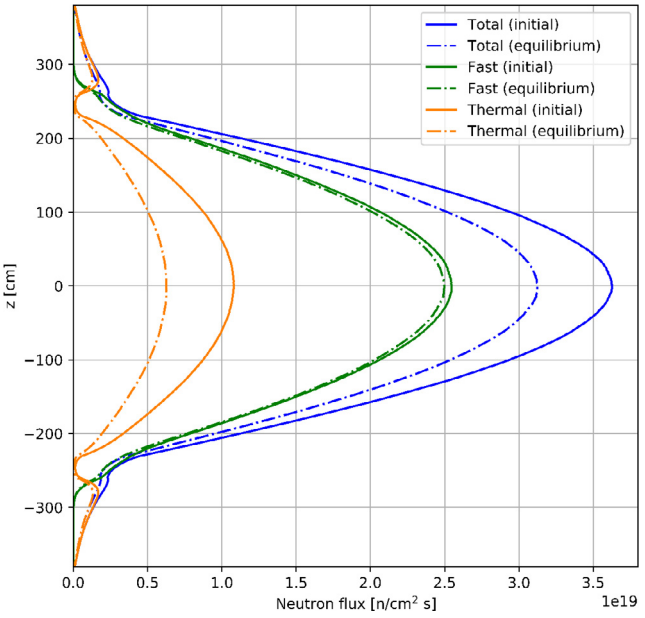

Fig. 16. Axial neutron flux distribution for initial and equilibrium fuel salt composition (the total flux confidence intervals $\pm\sigma$ are 0.6398% and 0.6199%, respectively).

(Sjöstrand et al., 1960). Moreover, additional fission products with a large thermal absorption cross-sections accumulate in the fuel during reactor operation. This leads to hardening of the neutron spectrum during reactor operation.

More changes in neutron flux shape and amplitude were observed in the inner core zone than in the outer zone for both fast and thermal neutrons. In the axial direction, thick graphite reflectors significantly reduce thermal neutron leakage – even for the harder spectrum at equilibrium state. In sum, the spectrum hardening phenomena during SD-TMSR operation must be carefully investigated when designing the reactivity control system.

5.5. Power and breeding distribution

Table 4 demonstrates the power fraction generated in each reactor core zone for initial and equilibrium fuel compositions.

Please cite this article as: O. Ashraf, A. Rykhlevskii, G. V. Tikhomirov et al., Whole core analysis of the single-fluid double-zone thorium molten salt reactor (SD-TMSR), Annals of Nuclear Energy, https://doi.org/10.1016/j.anucene.2019.107115

Table 4
Power generation fraction in different core zones for initial and equilibrium state.

Core region	Initial	Equilibrium
Inner zone	$83.625 \pm 0.383\%$	$87.833 \pm 0.267\%$
Outer zone	$16.375 \pm 0.897\%$	$12.167 \pm 0.973\%$

Fig. 17 demonstrates the normalized power distribution of the SD-TMSR quarter core for startup and equilibrium. The spectrum hardening during reactor operation results in considerably different power fractions at startup and equilibrium. For both the initial and equilibrium compositions, fission primarily occurs in the inner core zone ($R \lesssim 150$ cm). The spectrum hardening during reactor operation does not cause significant changes in fission power distribution but the power peak in the center of the core increased by approximately 43%. Even after reaching equilibrium fuel salt composition the inner core zone still generates the majority of the reactor's power.

Fig. 18 shows normalized neutron capture reaction rate distribution for ^{232}Th at equilibrium state. This distribution demonstrates spatial distribution of ^{233}U breeding in the core. First, ^{232}Th captures a neutron to form ^{233}Th. Then ^{233}Th β-decays to ^{233}Pa ($\tau_{1/2} \approx 21.83 min$), which β-decays to ^{233}U ($\tau_{1/2} \approx 27 d$). These distributions emphasize the Single-fluid Double-zone design's effectiveness for the SD-TMSR concept. In sum, spectral shifts during reactor operation do not cause significant changes in power nor in breeding distribution. Even after 20 years of operation, most of the power generation and ^{233}U production occurs in the inner core zone while the outer core zone works as reflector to reduce neutron leakage.

5.6. Temperature coefficient of reactivity

The temperature coefficient of reactivity is a crucial parameter for a reactor's safety and it must remain negative throughout the reactor lifetime. Table 5 summarizes temperature effects on reactivity calculated in this work for both initial and equilibrium fuel compositions, compared with the Li et al. (2018). By propagating the k_{eff} statistical error provided by SERPENT-2, uncertainty for each temperature coefficient was obtained. These values appear in Table 5. The main physical principle underlying the reactor temperature feedback is an expansion of heated material. When the fuel salt temperature increases, the density of the salt decreases (non-linearly), but the total volume of fuel salt in the core remains constant because of the graphite barrier. When the graphite temperature increases, the density of graphite decreases, creating additional space for fuel salt. To determine the temperature coefficients, the cross-section temperatures for the fuel and moderator were changed from 900 K to 1000 K. This study considered three different cases:

1. Fuel salt temperature rising from 900 K to 1000 K.
2. Graphite temperature rising from 900 K to 1000 K.
3. Whole reactor temperature rising from 900 K to 1000 K.

In the first case, changes in the fuel temperature only impact fuel density. The geometry is unchanged because the fuel is a liquid. However, when the moderator heats up, both the density and the geometry change due to thermal expansion of the solid

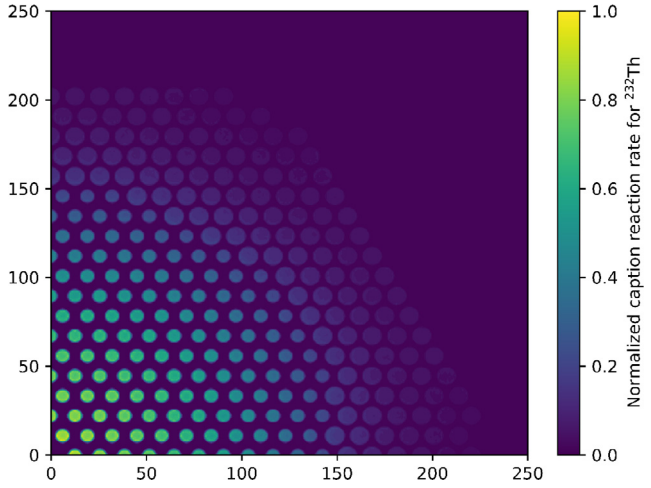

Fig. 18. Normalized ^{232}Th neutron capture reaction rate for equilibrium fuel salt composition.

Table 5
Temperature coefficients of reactivity for initial and equilibrium state.

Reactivity coefficient	Initial [pcm/K]	Equilibrium [pcm/K]	Reference (initial/equilibrium) (Li et al., 2018)
Fuel salt temperature	-4.44 ± 0.153	-5.12 ± 0.151	
Fuel salt density	$+1.45 \pm 0.149$	$+2.82 \pm 0.151$	
Total fuel salt	-3.41 ± 0.151	-2.67 ± 0.152	
Graphite temperature	$+2.26 \pm 0.152$	$+0.98 \pm 0.152$	
Total core	-1.19 ± 0.153	-2.27 ± 0.169	$-2.0/-1.8$

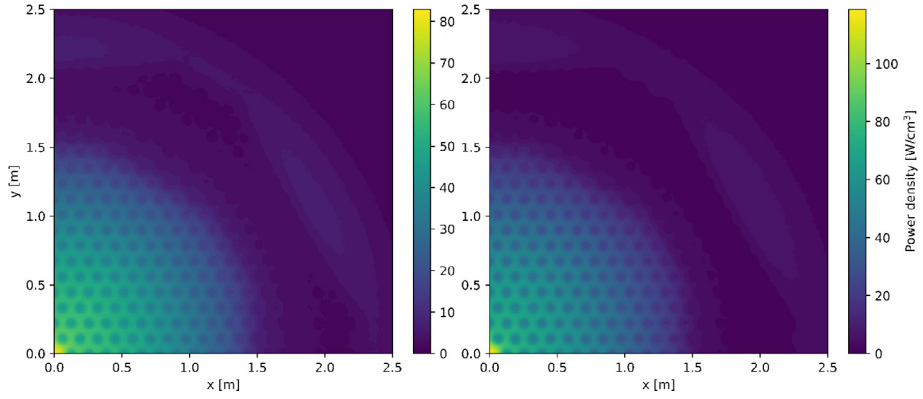

Fig. 17. Power density for initial and equilibrium fuel salt composition.

Please cite this article as: O. Ashraf, A. Rykhlevskii, G. V. Tikhomirov et al., Whole core analysis of the single-fluid double-zone thorium molten salt reactor (SD-TMSR), Annals of Nuclear Energy, https://doi.org/10.1016/j.anucene.2019.107115

graphite blocks and reflector. The graphite thermal expansion is not a dominating factor (Li et al., 2018), and herein we focus only on Doppler Effect for the graphite.

The Fuel Temperature Coefficient (FTC) is negative for both initial and equilibrium fuel compositions due to thermal Doppler broadening of the resonance capture cross-sections in the thorium. A small positive effect of fuel density on reactivity increases from +1.45 pcm/K at reactor startup to +2.88 pcm/K for equilibrium fuel composition, which negatively affects the FTC magnitude during reactor operation. The Moderator Temperature Coefficient (MTC) is positive for the startup composition and decreases during reactor operation because of spectrum hardening with fuel depletion. Finally, the total temperature coefficient of reactivity is negative for both cases, but decreases in magnitude during reactor operation due to spectral shift. These coefficients agree with earlier estimates for SD-TMSR (Li et al., 2018) and MSBR (Rykhlevskii et al., 2019, Rykhlevskii et al., 2017, Robertson, 1971).

Even after 20 years of operation, the total temperature coefficient of reactivity remains relatively large and negative during reactor operation (compared with the conventional Pressurized Water Reactor (PWR), which has temperature coefficient of about -1.71 pcm/$^{\circ}F \approx -3.08$ pcm/K (Forget et al., 2018), despite positive MTC, and allows excellent reactor stability and control. Additional analysis should be performed taking graphite moderator expansion into account, but material properties for SD-TMSR graphite are not available in published literature.

5.7. Six factor analysis

The effective multiplication factor can be expressed using the following formula:

$$k_{eff} = k_{inf} P_f P_t = \eta \epsilon p f P_f P_t$$

Table 6 summarizes the six factors for both initial and equilibrium fuel salt composition. Using SERPENT-2 built-in online reprocessing capabilities all six factors and their statistical uncertainties have been calculated at the beginning of operation and after 20 years of operation. The fast and thermal non-leakage probabilities and the thermal utilization factor (f) remain constant regardless of neutron spectrum hardening during operation. In contrast, the neutron reproduction factor (η), resonance escape probability (p), and fast fission factor (ϵ) differ notably between initial and equilibrium state. The neutron spectrum is soft at the beginning of reactor life (Fig. 14), but neutron spectrum hardening causes the fast fission factor to grow throughout the core's lifetime. Conversely, the resonance escape probability decreases during reactor operation. The neutron reproduction factor increases during reactor operation due to accumulation of fissile plutonium isotopes, which produce more neutrons per fission (ν). This six factors' evolution agrees with previously determined evolution parameters for a similar single-fluid double-zone MSBR (Rykhlevskii et al., 2019; Park et al., 2015).

Table 6
Six factors for the SD-TMSR model for initial and equilibrium fuel composition.

Factor	Initial	Equilibrium
Neutron reproduction factor (η)	1.2904±1.7E−4	1.4186±1.7E−4
Thermal utilization factor (f)	0.9703±3.3E−5	0.9784±3.2E−5
Resonance escape probability (p)	0.5399±1.3E−4	0.4357±1.6E−4
Fast fission factor (ϵ)	1.4964±1.5E−5	1.6643±1.8E−5
Fast non-leakage probability (P_f)	0.9999±1.5E−7	0.9999±1.1E−7
Thermal non-leakage probability (P_t)	1.0000±0.0E−0	1.0000±0.0E−0

Table 7
Major fuel cycle performance parameters in comparison with Li et al. (2018).

Parameters	SERPENT-2	MSR-RS code (Li et al., 2018)
Initial inventory of ^{233}U, t	1.3	1.27
Initial k_{eff}	1.00469 ± 0.00035	1.010 ± 0.005
Initial BR	1.11658 ± 0.00060	1.104
TCR(initial/equilibrium), pcm/K	−1.19/−2.27	−2.0/−1.8
The net production of ^{233}U during 60 years of operation, t	1.77	4
Doubling time for ^{233}U, years	26	16

5.8. Validation with other codes

The results from the present work have been compared with Li et al. (2018). Li and colleagues used the in–house tool MSR-RS based on SCALE 6.1 and applied it to the SD-TMSR. This code package performs multi-step burnup computations. After each step, it interrupts the simulation, removes FPs, refuels ^{233}U, and runs the next depletion simulation step. In contrast, the present paper adopted the MSR burnup routine to simulate continuous online reprocessing and refueling of the same reactor (i.e. SD-TMSR). Both methods applied the same reprocessing period, namely: extraction of the gaseous FPs and non-dissolved metals in 30 s and removing of soluble FPs and Pa within 10.59 days (i.e. 5 m^3/d)). In addition, both methods extracted ^{233}Pa out of the active core and reinjected the produced ^{233}U into the core for criticality as soon as possible. Table 7 compares fuel performance and safety parameters obtained by each method.

6. Conclusion

The present work contributes to a better understanding of MSRs; it emphasizes the SERPENT-2 Monte Carlo code's ability to analyze the whole core model of the SD-TMSR with online reprocessing and refueling. The conclusions are listed as follows:

- During burnup, reactor criticality was maintained by adjusting the feed rates of ^{233}U and ^{232}Th. The mean value of ^{233}U and ^{232}Th feed rates were 1.77 and 2.21 kg/d, respectively. Meanwhile, the total fuel mass variation was less than 0.1%. Additionally, the inventory of Pa, Pu, and MA in the fuel salt during the reactor operation has been investigated to determine the composition at equilibrium.
- After 20 years of operation, the neutron spectrum remains almost constant. Consequently, the equilibrium is achieved at 20 years, at which point the neutron spectrum has hardened due to the accumulation of plutonium and strong thermal neutron absorbers in the core throughout burnup.
- We compared the operational and safety parameters of the SD-TMSR at both initial and equilibrium states. The total coefficient of reactivity was found to be negative at a value of -1.19 ± 0.153 pcm/K and -2.27 ± 0.169 pcm/K for the initial and equilibrium states, respectively. These results agree with published data (Li et al., 2018).
- Although the net production of ^{233}U increased with burnup (reached about 1.77 t at the end of the period), it was found that it takes 26 years to double the ^{233}U inventory. Further design optimization could reduce the doubling time for ^{233}U production.

Future work

The authors intend to compare the present results and results from SaltProc batch-wise code (Rykhlevskii et al., 2019) in future

Please cite this article as: O. Ashraf, A. Rykhlevskii, G. V. Tikhomirov et al., Whole core analysis of the single-fluid double-zone thorium molten salt reactor (SD-TMSR), Annals of Nuclear Energy, https://doi.org/10.1016/j.anucene.2019.107115

work. Moreover, they will consider the delayed neutron precursor drift. Future work will also consider the benchmark study based on other codes and models. The authors intend to conduct a sensitivity study to evaluate the impact of the radial reflector material and its thickness. In addition, they will study the impact of FPs removal (i.e. only reprocessing without refueling) on reactivity and neutron economy.

Declaration of Competing Interest

The authors declare that they have no known competing financial interests or personal relationships that could have appeared to influence the work reported in this paper.

Acknowledgments

Osama Ashraf would like to thank the Egyptian Ministry of Higher Education (MoHE), as well as MEPhI's Competitiveness Program for providing financial support for this research. The facility and tools needed to conduct this work were supported by MEPhI.

The authors contributed to this work as described below.

Osama Ashraf conceived and designed the simulations, wrote the paper, prepared figures and/or tables, performed the computation work, and reviewed drafts of the paper.

Andrei Rykhlevskii conceived and designed the simulations, wrote the paper, prepared figures and/or tables, performed the computation work, and reviewed drafts of the paper. Andrei Rykhlevskii is supported by DOE ARPA-E MEITNER program award DE-AR0000983.

G.V. Tikhomirov directed and supervised the work, conceived and designed the simulations and reviewed drafts of the paper. Prof. Tikhomirov is supported by Rosatom, he is Deputy Director of the Institute of Nuclear Physics and Engineering MEPhI. Board member of Nuclear society of Russia.

Kathryn D. Huff supervised the work, conceived and contributed to conception of the simulations, and reviewed drafts of the paper. Prof. Huff is supported by the Nuclear Regulatory Commission Faculty Development Program, the National Center for Supercomputing Applications, the NNSA Office of Defense Nuclear Nonproliferation R&D through the Consortium for Verification Technologies and the Consortium for Nonproliferation Enabling Capabilities, the International Institute for Carbon Neutral Energy Research (WPI-I2CNER), sponsored by the Japanese Ministry of Education, Culture, Sports, Science and Technology, and DOE ARPA-E MEITNER program award DE-AR0000983.

This research is part of the Blue Waters sustained-petascale computing project, which is supported by the National Science Foundation (awards OCI-0725070 and ACI-1238993) and the state of Illinois. Blue Waters is a joint effort of the University of Illinois at Urbana-Champaign and its National Center for Supercomputing Applications

Appendix A. Supplementary data

Supplementary data associated with this article can be found, in the online version, athttps://doi.org/10.1016/j.anucene.2019.107115.

References

Ade, B., 2012. SCALE/TRITON Primer: A Primer for Light Water Reactor Lattice Physics Calculations. United States Nuclear Regulatory Commission, Office of Nuclear Regulatory.

Ashraf, O., Smirnov, A., Tikhomirov, G., 2018. Nuclear fuel optimization for molten salt fast reactor. J. Phys.: Conf. Ser. 1133, 012026. https://doi.org/10.1088/1742-6596/1133/1/012026. IOP Publishing.

Aufiero, M., Cammi, A., Fiorina, C., Leppänen, J., Luzzi, L., Ricotti, M.E., 2013. An extended version of the serpent-2 code to investigate fuel burn-up and core material evolution of the molten salt fast reactor. J. Nucl. Mater. 441 (1–3), 473–486.

Bergel'son, B., Gerasimov, A., Tikhomirov, G., Tszin'khun, L., 2004. Mode of self-sufficiency by the uranium-233 for heavy-water power reactor of Candu type. Atomnaya Ehnergiya 97 (4), 269–275.

Bergelson, B.R., Gerasimov, A.S., Tikhomirov, G.V., 2008. Optimization of the self-sufficient thorium fuel cycle for Candu power reactors. Nucl. Technol. Radiat. 23, 38.

Betzler, B.R., Powers, J.J., Worrall, A., 2017. Molten salt reactor neutronics and fuel cycle modeling and simulation with scale. Ann. Nucl. Energy 101, 489–503.

Boussier, H., Delpech, S., Ghetta, V., Heuer, D., Holcomb, D., Ignatiev, V., Merle-Lucotte, E., Serp, J., 2012. The molten salt reactor in generation. iv: Overview and perspectives. In: Proceedings of the Generation4 International Forum Symposium, San Diego, USA.

Briesmeister, J.F. et al., 2000. Mcnptm-a general monte carlo n-particle transport code, Version 4C, LA-13709-M. Los Alamos National Laboratory. 2.

Bucholz, J., 1982. Scale: A Modular Code System for Performing Standardized Computer Analyses for Licensing Evaluation. Oak Ridge National Laboratory. Tech. rep.

Dastur, A., Meneley, D., Buss, D., 1995. Thorium cycle options in Candu reactors. Global, 1995.

Davidson, G.G., Pandya, T.M., Johnson, S.R., Evans, T.M., Isotalo, A.E., Gentry, C.A., Wieselquist, W.A., 2018. Nuclide depletion capabilities in the shift monte carlo code. Ann. Nucl. Energy 114, 259–276.

DeHart, M.D., Ulses, A., 2006. In: Proc. of PHYSOR-2006, pp. 10–14.

DOE, US, 2002. A technology roadmap for generation iv nuclear energy systems, pp. 48–52.

Engel, J., Bauman, H., Dearing, J., Grimes, W., McCoy Jr, H., 1979. Development Status and Potential Program for Development of Proliferation-resistant Molten-salt Reactors. Oak Ridge National Lab. Tech. rep.

Fiorini, G., Leahy, T., 2009. Basis for the safety approach for design and assessment of generation iv nuclear systems.

Forget, B., Smith, K., Kumar, S., Rathbun, M., Liang, J., 2018. Integral Full Core Multi-physics PWR Benchmark with Measured Data. Massachusetts Institute of Technology. Tech. rep.

Haeck, W., 2012. Vesta user's manual version 2.1.0, dsusec/t/2011-81, DSUSEC/T/2011-81 114, 259–276. .

Hargraves, R., Moir, R., 2010. Liquid fluoride thorium reactors: an old idea in nuclear power gets reexamined. Am. Sci. 98 (4), 304–313.

Haubenreich, P.N., Engel, J., 1970. Experience with the molten-salt reactor experiment. Nucl. Appl. Technol. 8 (2), 118–136.

Isotalo, A., Pusa, M., 2016. Improving the accuracy of the Chebyshev rational approximation method using substeps. Nucl. Sci. Eng. 183 (1), 65–77.

Jeong, Y., Park, J., Lee, H.C., Lee, D., 2016. Equilibrium core design methods for molten salt breeder reactor based on two-cell model. J. Nucl. Sci. Technol. 53 (4), 529–536. https://doi.org/10.1080/00223131.2015.1062812. arXiv: https://doi.org/10.1080/00223131.2015.1062812.

Jiang, M., Xu, H., Dai, Z., 2012. Advanced fission energy program-TMSR nuclear energy system. Bull. Chin. Acad. Sci. 27 (3), 366–374.

Leppänen, J., Pusa, M., Viitanen, T., Valtavirta, V., Kaltiaisenaho, T., 2013. The serpent monte carlo code: status, development and applications in 2013. In: SNA+ MC 2013-Joint International Conference on Supercomputing in Nuclear Applications+ Monte Carlo. EDP Sciences, p. 06021.

Li, X., Cai, X., Jiang, D., Ma, Y., Huang, J., Zou, C., Yu, C., Han, J., Chen, J., 2015. Analysis of thorium and uranium based nuclear fuel options in fluoride salt-cooled high-temperature reactor. Prog. Nucl. Energy 78, 285–290.

Li, G., Zou, Y., Yu, C., et al., 2017. Model optimization and analysis of Th-U breeding based on MSFR. Nucl. Technol. 40. 020603–020603.

Li, G.C., Cong, P., Yu, C.G., Zou, Y., Sun, J.Y., Chen, J.G., Xu, H.J., 2018. Optimization of Th-U fuel breeding based on a single-fluid double-zone thorium molten salt reactor. Prog. Nucl. Energy 108, 144–151. https://doi.org/10.1016/j.pnucene.2018.04.017. URL: http://www.sciencedirect.com/science/article/pii/S0149197018300970.

Locatelli, G., Mancini, M., Todeschini, N., 2013. Generation iv nuclear reactors: current status and future prospects. Energy Policy 61, 1503–1520.

Mathieu, L., Heuer, D., Brissot, R., Garzenne, C., Le Brun, C., Lecarpentier, D., Liatard, E., Loiseaux, J.-M., Meplan, O., Merle-Lucotte, E., et al., 2006. The thorium molten salt reactor: moving on from the msbr. Prog. Nucl. Energy 48 (7), 664–679.

Merle-Lucotte, E., Mathieu, L., Heuer, D., Ghetta, V., Brissot, R., Brun, C.L., Liatard, E., 2008. Influence of the processing and salt composition on the thorium molten salt reactor. Nucl. Technol. 163 (3), 358–365.

Merle-Lucotte, E., Heuer, D., Allibert, M., Doligez, X., Ghetta, V., 2009. Minimizing the fissile inventory of the molten salt fast reactor. In: Advances in Nuclear Fuel Management IV (ANFM IV). American Nuclear Society.

Mourogov, A., Bokov, P., 2006. Potentialities of the fast spectrum molten salt reactor concept: Rebus-3700. Energy Convers. Manage. 47 (17), 2761–2771.

Nagy, K., Kloosterman, J., Lathouwers, D., Van der Hagen, T., 2011. New breeding gain definitions and their application to the optimization of a molten salt reactor design. Ann. Nucl. Energy 38 (2–3), 601–609.

Nagy, K., Kloosterman, J., Lathouwers, D., Van der Hagen, T., 2012. The effects of core zoning on the graphite lifespan and breeding gain of a moderated molten salt reactor. Ann. Nucl. Energy 43, 19–25.

Nuttin, A., Heuer, D., Billebaud, A., Brissot, R., Le Brun, C., Liatard, E., Loiseaux, J.-M., Mathieu, L., Meplan, O., Merle-Lucotte, E., et al., 2005. Potential of thorium

molten salt reactors detailed calculations and concept evolution with a view to large scale energy production. Progr. Nucl. Energy 46 (1), 77–99.

Park, J., Jeong, Y., Lee, H.C., Lee, D., 2015. Whole core analysis of molten salt breeder reactor with online fuel reprocessing. Int. J. Energy Res. 39 (12), 1673–1680. https://doi.org/10.1002/er.3371.

Pettersen, E.E., Mikityuk, K., 2016. Coupled Multi-physics Simulations of the Molten Salt Fast Reactor using Coarse-mesh Thermal-hydraulics and Spatial Neutronics. Universite Paris-Saclay.

Pioro, I., 2016. Handbook of Generation IV Nuclear Reactors. Woodhead Publishing.

Robertson, R., 1965. MSRE design and operations report. Part i. Description of reactor design. Oak Ridge National Laboratory, Tenn. Tech. rep.

Robertson, R.C., 1971. Conceptual Design Study of a Single-Fluid Molten-Salt Breeder Reactor. Tech. Rep. ORNL-4541, comp.; Oak Ridge National Laboratory, Tenn. (Jan. 1971).http://www.osti.gov/scitech/biblio/4030941. .

Rosenthal, M., Kasten, P., Briggs, R., 1970. Molten-salt reactors-history, status, and potential. Nucl. Appl. Technol. 8 (2), 107–117.

Rykhlevskii, A., Lindsay, A., Huff, K.D., 2017. Online reprocessing simulation for thorium-fueled molten salt breeder reactor. In: Transactions of the American Nuclear Society. American Nuclear Society, Washington, DC, United States.

Rykhlevskii, A., Lindsay, A., Huff, K.D., 2017. Full-core analysis of thorium-fueled Molten Salt Breeder Reactor using the SERPENT 2 Monte Carlo code. In: Transactions of the American Nuclear Society. American Nuclear Society, Washington, DC, United States.

Rykhlevskii, A., Bae, J.W., Huff, K.D., 2019. Modeling and simulation of online reprocessing in the thorium-fueled molten salt breeder reactor. Ann. Nucl. Energy 128, 366–379. https://doi.org/10.1016/j.anucene.2019.01.030.

Serp, J., Allibert, M., Beneš, O., Delpech, S., Feynberg, O., Ghetta, V., Heuer, D., Holcomb, D., Ignatiev, V., Kloosterman, J.L., et al., 2014. The molten salt reactor (MSR) in generation. IV: Overview and perspectives. Prog. Nucl. Energy 77, 308–319.

Sjöstrand, N.G., Story, J.S., 1960. Cross sections and neutron yields for U-233, U-235 and Pu-239 at 2200 m/sec. AB Atomenergi. Tech. rep.

Taube, M., 1978. Fast Reactors Using Molten Chloride Salts as Fuel. INFCE (Switzerland). Tech. rep.

Trellue, H.R., Poston, D.I., 1999. User's manual, version 2.0 for monteburns, version 5b, preprint LA-UR-99-4999, LANL. .

Zhang, D., Liu, L., Liu, M., Xu, R., Gong, C., Zhang, J., Wang, C., Qiu, S., Su, G., 2018. Review of conceptual design and fundamental research of molten salt reactors in China. Int. J. Energy Res. 42 (5), 1834–1848.

Zou, C., Cai, X., Jiang, D., Yu, C., Li, X., Ma, Y., Han, J., Chen, J., 2015. Optimization of temperature coefficient and breeding ratio for a graphite-moderated molten salt reactor. Nucl. Eng. Des. 281, 114–120. https://doi.org/10.1016/j.nucengdes.2014.11.022. URL: http://www.sciencedirect.com/science/article/pii/S0029549314006323.

Please cite this article as: O. Ashraf, A. Rykhlevskii, G. V. Tikhomirov et al., Whole core analysis of the single-fluid double-zone thorium molten salt reactor (SD-TMSR), Annals of Nuclear Energy, https://doi.org/10.1016/j.anucene.2019.107115